Two flavor color superconductivity in nonlocal chiral quark models

R. S. Duhau[a], A. G. Grunfeld[a] and N.N. Scoccola[a,b,c]

[a] *Physics Department, Comisión Nacional de Energía Atómica, Av.Libertador 8250, (1429) Buenos Aires, Argentina.*
[b] *CONICET, Rivadavia 1917, (1033) , Argentina.*
[c] *Universidad Favaloro, Solís 453, (1078) Buenos Aires, Argentina*

Abstract

We study the competence between chiral symmetry restoration and two flavor color superconductivity (2SC) using a relativistic quark model with covariant nonlocal interactions. We consider two different nonlocal regulators: a Gaussian regulator and a Lorentzian regulator. We find that although the phase diagrams are qualitative similar to those obtained using models with local interactions, in our case the superconducting gaps at medium values of the chemical potential are larger. Consequently, we obtain that in that region the critical temperatures for the disappearance of the 2SC phase might be of the order of 100-120 MeV. We also find that for ratios of the quark-quark and quark-antiquark couplings somewhat above the standard value 3/4, the end point and triple point in the $T-\mu$ phase diagram meet and a phase where both the chiral and diquark condensates are non-negligible appears.

PACS numbers: 12,39.Ki.12.38.Mh.

I Introduction

The understanding of the QCD phase diagram has become one of the most interesting issues in the physics of strong interactions. Such phase diagram is relevant to phenomena in the early universe, in the interior of neutron stars and in relativistic heavy ion collisions. Already in the seventies it was suggested that there should be two distinct phases: a low temperature and density phase in which quarks and gluons are confined within hadrons and chiral symmetry is broken, and a high temperature and density phase (the so-called quark-gluon plasma) in which these particles are deconfined and chiral symmetry is restored. Although the possible existence of other phases (e.g. the color superconducting phase) was also suggested quite long ago[1], this two-phase structure became the standard picture of the QCD phase diagram for more than two decades. In recent years, however, it has been established that at low temperatures and medium densities several other phases might appear (see e.g. Ref.[2] for recent reviews). In particular, for the case of two light flavors it has been shown that there should be a non-negligible region in the QCD phase diagram where strongly interacting matter is a color superconductor (2SC phase)[3]. Unfortunately, due to difficulties in dealing with finite chemical potential, ab initio calculations (as e.g. lattice QCD) are not yet able to provide a detailed knowledge of the QCD phase diagram[4]. Thus, most theoretical approaches are based on the use of effective models of QCD. Among them, the Nambu-Jona-Lasinio model[5] is one of the most popular. In this model the quark fields interact via local

four point vertices which are subject to chiral symmetry. If such interaction is strong enough, chiral symmetry is spontaneously broken at zero temperature and density, and pseudoscalar Goldstone bosons appear. It has been shown by many authors that when the temperature and/or density increase, the chiral symmetry is restored[6]. When effective quark-quark interactions are added to the effective lagrangian other phases also appear[7]. As an improvement on the local NJL model, some covariant nonlocal extensions have been studied in the last few years[8]. Nonlocality arises naturally in the context of several successful approaches to low-energy quark dynamics as, for example, the instanton liquid model[9] and the Schwinger-Dyson resummation techniques[10]. It has been also argued that nonlocal covariant extensions of the NJL model have several advantages over the local scheme. Several studies[11, 12, 13] have shown that these nonlocal models provide a satisfactory description of the hadron properties at zero temperature and density. Recently[14], the characteristics of the chiral phase transition have been investigated within this kind of models. The aim of the present work is to extend such studies to the case in which a superconducting phase can appear.

This article is organized as follows. In Sec. II we introduce the model and formalism. Our results for some specific nonlocal regulators are presented in Sec. III. In Sec. IV we analyze the dependence of our results on the strength of the diquark correlations. Finally, in Sec. V we give our conclusions.

II The formalism

Let us begin by stating the Euclidean action for the nonlocal chiral quark model in the case of two light flavors and $SU(2)$ isospin symmetry. For the purpose of the present study it is enough to only consider interactions in the scalar quark-antiquark and quark-quark channels. Thus, one has

$$\begin{aligned} S_E &= \int d^4x \left\{ \bar{\psi}(x) \left(-i\partial\!\!\!/ + m_c\right) \psi(x) \right. \\ &\left. -\frac{G}{2} \left[\bar{q}(x)\ q(x)\right]^2 - \frac{H}{2} \left[\bar{q}(x)\ i\gamma_5\tau_2\lambda_2\ q_C(x)\right] \left[\bar{q}_C(x)\ i\gamma_5\tau_2\lambda_2\ q(x)\right] \right\} , \end{aligned} \tag{1}$$

where m_c is the current quark mass and τ_2 and λ_2 are Pauli and Gell-Mann matrices corresponding to the flavor and color groups, respectively. The delocalized quark fields $q(x)$ are defined in terms of the quark fields $\psi(x)$ as

$$q(x) = \int d^4y\ r(x-y)\ \psi(y) \tag{2}$$

where the function $r(x-y)$ is a nonlocal regulator. It can be translated into momentum space,

$$r(x-z) = \int \frac{d^4p}{(2\pi)^4}\ e^{-i(x-z)p}\ r(p)\ . \tag{3}$$

Lorentz invariance implies that $r(p)$ can only be a function of p^2. Hence we will use for the Fourier transform of the regulator the form $r(p^2)$ from now on. In addition, in Eq.(1) we have used

$$q_C(x) = \gamma_2\gamma_4\ \bar{q}^{\,t}(x) \qquad ; \qquad \bar{q}_C(x) = q^{\,t}(x)\ \gamma_2\gamma_4. \tag{4}$$

The partition function for the model is defined as

$$\mathcal{Z} = \int \mathcal{D}\bar{\psi}\mathcal{D}\psi\ e^{-S_E(\mu,T)}\ , \tag{5}$$

where the Euclidean action at finite temperature T and chemical potential μ is obtained from Eq. (1) by going to momentum space and performing the replacement

$$\int \frac{d^4p}{(2\pi)^4}\, F(\vec{p},p_4) \quad \to \quad T\sum_{n=-\infty}^{\infty}\int \frac{d^3\vec{p}}{(2\pi)^3}\, F(\vec{p},\omega_n - i\mu)\,, \tag{6}$$

where ω_n are the Matsubara frequencies corresponding to fermionic modes, $\omega_n = (2n+1)\pi T$. As in Ref.[14] we are assuming here that the quark interactions only depend on the temperature and chemical potential through the argument of the regulators. To proceed it is convenient to perform a standard bosonization of the theory. Thus, we introduce the sigma meson field σ and the scalar diquark field Δ and integrate out the quark fields. In what follows we will work within the mean field approximation (MFA), in which these bosonic fields are expanded around their vacuum expectation values $\bar{\sigma}$ and $\bar{\Delta}$ and the corresponding fluctuations neglected. Within this approximation and employing the Nambu-Gorkov formalism, the mean field thermodynamical potential per unit volume reads

$$\Omega^{MFA} = -\frac{T}{V}\,\ln \mathcal{Z}^{MFA} = \frac{\bar{\sigma}^2}{2G} + \frac{|\bar{\Delta}|^2}{2H} - T\sum_{n=-\infty}^{\infty}\int \frac{d^3\vec{p}}{(2\pi)^3}\,\frac{1}{2}Tr\ln\left[\frac{1}{T}\,S^{-1}(\bar{\sigma},\bar{\Delta})\right] \tag{7}$$

where Tr stands for the trace over the Dirac, flavor, color and Nambu-Gorkov bispinor indexes. The inverse propagator $S^{-1}(\bar{\sigma},\bar{\Delta})$ is

$$S^{-1}(\bar{\sigma},\bar{\Delta}) = \begin{pmatrix} -\vec{p}\cdot\vec{\gamma} - (\omega_n - i\mu)\,\gamma^4 + \Sigma_p & i\gamma_5\tau_2\lambda_2\Delta_p \\ i\gamma_5\tau_2\lambda_2\Delta_p^* & -\vec{p}\cdot\vec{\gamma} - (\omega_n + i\mu)\,\gamma^4 + \Sigma_p{}^* \end{pmatrix}\,, \tag{8}$$

where

$$\Sigma_p = m_c + \bar{\sigma}\; r_p^2 \qquad ; \qquad \Delta_p = \bar{\Delta}\;|r_p|^2 \tag{9}$$

and $r_p \equiv r\left(\vec{p}^{\,2} + (\omega_n - i\mu)^2\right)$. After some straightforward algebra Ω^{MFA} can be more explicitly expressed as

$$\begin{aligned}\Omega^{MFA} \;=\; & \frac{\bar{\sigma}^2}{2G} + \frac{|\bar{\Delta}|^2}{2H} - \\ & 2\;T\sum_{n=-\infty}^{\infty}\int \frac{d^3\vec{p}}{(2\pi)^3}\left\{2\ln\left[\frac{\left(A_p + |\Delta_p|^2\right)^2 - B_p - 4C_p^2}{T^4}\right] + \ln\left[\frac{A_p^2 - B_p - 4C_p^2}{T^4}\right]\right\}\end{aligned} \tag{10}$$

where,

$$A_p = \omega_n^2 + \vec{p}^{\,2} + \mu^2 + |\Sigma_p|^2, \qquad B_p = 4\vec{p}^{\,2}\left(\mu^2 + \mathrm{Im}^2\Sigma_p\right), \qquad C_p = \mu\;\mathrm{Re}\Sigma_p + \omega_n\;\mathrm{Im}\Sigma_p\;. \tag{11}$$

For finite values of the current quark mass, Ω^{MFA} turns out to be divergent. The regularization procedure used here amounts to define

$$\Omega^{MFA}_{(reg)} = \Omega^{MFA} - \Omega^{free} + \Omega^{free}_{(reg)}, \tag{12}$$

where $\Omega^{free}_{(reg)}$ is the regularized expression for the thermodynamical potential of a free fermion gas,

$$\Omega^{free}_{(reg)} = -12\;T\int \frac{d^3\vec{p}}{(2\pi)^3}\;\left[\ln\left(1 + e^{-\left(\sqrt{\vec{p}^2+m_c^2}-\mu\right)/T}\right) + \ln\left(1 + e^{-\left(\sqrt{\vec{p}^2+m_c^2}+\mu\right)/T}\right)\right]. \tag{13}$$

The mean field values $\bar{\sigma}$ and $\bar{\Delta}$ are obtained from the coupled pair of gap equations

$$\frac{d\Omega^{MFA}_{(reg)}}{d\bar{\sigma}} = 0 \qquad , \qquad \frac{d\Omega^{MFA}_{(reg)}}{d\bar{\Delta}} = 0 \ . \tag{14}$$

The explicit form of these equations is

$$\begin{aligned} 0 &= \bar{\sigma} - 16\ G\ T \sum_{n=-\infty}^{\infty} \int \frac{d^3\vec{p}}{(2\pi)^3} \left\{ \frac{(A_p + |\Delta_p|^2)E_p - F_p - 2C_pG_p}{(A_p + |\Delta_p|^2)^2 - B_p - 4\ C_p^2} + \frac{A_pE_p - F_p - 2C_pG_p}{2\left(A_p^2 - B_p - 4C_p^2\right)} \right\} \ , \\ 0 &= |\bar{\Delta}| \left[1 - 16\ H\ T \sum_{n=-\infty}^{\infty} \int \frac{d^3\vec{p}}{(2\pi)^3} \left\{ |r_p|^4\ \frac{A_p + |\Delta_p|^2}{(A_p + |\Delta_p|^2)^2 - B_p - 4\ C_p^2} \right\} \right] , \end{aligned} \tag{15}$$

where, in addition to the definitions given in Eq.(11), we have used

$$E_p = \mathrm{Re}\Sigma_p\ \mathrm{Re}\ r_p^2 + \mathrm{Im}\Sigma_p\ \mathrm{Im}\ r_p^2 \ , \qquad F_p = 2\ \vec{p}^{\ 2}\ \mathrm{Im}\Sigma_p\ \mathrm{Im}\ r_p^2 \ , \qquad G_p = \mu\ \mathrm{Re}\ r_p^2 + \omega_n\ \mathrm{Im}\ r_p^2 \ . \tag{16}$$

It should be noticed that, in general, there might be regions for which there are more than one solution for each value of T and μ. In such regions we identify the stable solution by requiring it to be an overall minimum of the potential.

Given the thermodynamic potential the expressions for all other relevant quantities can be easily derived. For each flavor the quark-antiquark condensate $\langle\bar{\psi}\psi\rangle$ and the quark density ρ_q are given by

$$\langle\bar{\psi}\psi\rangle = \frac{\partial\Omega^{MFA}_{(reg)}}{\partial m_c} \qquad , \qquad \rho_q = -\frac{\partial\Omega^{MFA}_{(reg)}}{\partial\mu} \ . \tag{17}$$

In the case of the quark-quark condensate an extra source term $-\xi\ \bar{\psi}_C(x) i\gamma_5\tau_2\lambda_2\psi(x)$ has to be added to the effective action. It is easy to see that this leads to a thermodynamic potential $\Omega_{MFA}(\xi)$ which has the form given in Eq.(10) but where Δ_p has been replaced by $\Delta_p - \xi$. Then, we get

$$\langle\psi\psi\rangle = -\left.\frac{\partial\Omega^{MFA}_{(reg)}(\xi)}{\partial\xi}\right|_{\xi=0} \ . \tag{18}$$

Finally, a magnitud which is important to determine the characteristic of the chiral phase transition is the chiral susceptibility χ. It can be calculated as

$$\chi = -\frac{\partial^2\Omega^{MFA}_{(reg)}}{\partial m_c^2} = -\frac{\partial\langle\bar{\psi}\psi\rangle}{\partial m_c} \ . \tag{19}$$

III Numerical results for different regulators

In this section we concentrate on the numerical results obtained for two different regulators often used in the literature: the Gaussian regulator and the Lorentzian regulator. In each case we have considered G, m_c and Λ as input parameters fixed so as to reproduce the phenomenological values of the chiral condensate, pion mass and pion decay constant at vanishing temperature and densities[11, 14]. Moreover, we have set $H/G = 3/4$ as implied by, for example, OGE interactions [3, 7]. The dependence of our results on this ratio will be discussed in the following section.

III.1 Gaussian regulator

In this case the regulator is given by

$$r(p^2) = \exp(-p^2/2\Lambda^2), \tag{20}$$

where Λ plays the role of a cut-off parameter. We have considered two different sets of parameters. Set I corresponds to $G = 50\ GeV^{-2}$, $m_c = 10.5\ MeV$ and $\Lambda = 627\ MeV$ while Set II to $G = 30\ GeV^{-1}$, $m = 7.7\ MeV$ and $\Lambda = 760\ MeV$. Although for both sets the zero temperature and density properties mentioned above are well reproduced, in the case of Set I the quark propagator has no purely real poles while for Set II it does. Thus, following Ref.[11], Set I might be interpreted as a confining one, since quarks cannot materialize on-shell in Minkowski space.

The mean field values $\bar{\sigma}$ and $\bar{\Delta}$ as a function of μ and T are obtained by numerically solving Eqs.(15). The corresponding results as a function of μ for various values of T are displayed in Fig.1, where left panels correspond to Set I while right ones to Set II. It can be seen that, for small values of T and μ (full lines in Fig.1), the system is in the chiral phase for which $\bar{\sigma} \neq 0$ and $\bar{\Delta} = 0$. If we increase μ keeping T fixed, at some critical value of μ there is sudden drop of $\bar{\sigma}$ and a simultaneous sudden increase in $\bar{\Delta}$ so that we get into the 2SC phase characterized by $\bar{\sigma} \cong 0$ and $\bar{\Delta} \neq 0$. In particular, the values of the diquark gap at the critical chemical potential and $T = 0$ can be found in Table 1. If we repeat the process with a higher value of T something similar happens until we reach the "triple point" (3P). For temperatures slightly higher than T_{3P} (dashed lines in Fig.1) the sudden drop in $\bar{\sigma}$ and the increase $\bar{\Delta}$ start to happen at two different values of μ. Between these values of μ we have $\bar{\sigma} \cong 0$ and $\bar{\Delta} = 0$. Moreover there is no discontinuity in the behavior of $\bar{\Delta}$ as a function of μ. For temperatures above the "end point" (EP) the discontinuity in $\bar{\sigma}$ also disappears (dotted lines in Fig.1). Finally for temperatures above the critical temperature for $\mu = 0$, $T_c(\mu = 0)$, we get $\bar{\sigma} \cong 0$ for all values of μ. In the region corresponding to the crossover the transition point is defined by the point at which the chiral susceptibility χ has a maximum. The positions of the different critical points are summarized in Table 1. Also shown in Fig.1 are the corresponding quiral $\langle\bar{\psi}\psi\rangle$ and diquark $\langle\psi\psi\rangle$ condensates. Their behavior is quite similar to those of the mean field values $\bar{\sigma}$ and $\bar{\Delta}$, respectively. It is worthwhile to mention that the fact that the chiral condensate approaches some positive value for large values of μ is due to the substraction scheme used to regularize the thermodynamical potential, Eq.(12). In fact, it is not difficult to see that for finite values of m_c the regularized free thermodynamical potential $\Omega^{free}_{(reg)}$, Eq.(13), has such behavior.

The corresponding phase diagrams are displayed in Fig.2. Again left panels correspond to Set I and right ones to Set II. On the other hand, the upper panels correspond to the phase diagrams in the $T - \mu$ plane and the lower ones to the diagrams in the $T - \rho/\rho_0$ plane, where the nuclear matter density $\rho_0 = 1.3 \times 10^6 MeV$. In all the cases we have indicated with full lines the first order transition lines, with dashed lines the second order transition lines and with dotted lines the lines corresponding to the crossover between the chiral phase and the weakly interacting quark phase.

As it is clear from the $T - \mu$ phase diagrams, at the triple point the three phases can coexist. It is interesting to remark that for values of the chemical potential below μ_{3P} the transition line (both the first order and crossover sections) coincides exactly with that obtained in the absence of diquark correlations ($H = 0$). On the other hand, for $\mu > \mu_{3P}$ the first order transition line is different from that obtained in Ref.[14]. This is more clearly seen in the corresponding $T - \rho/\rho_0$ diagrams. There we have indicated with dash-dotted line the first order transition line corresponding to $H = 0$. As

we observed the existence of diquark correlations increases the size of the mixed phase. Note that for $T < T_{3P}$ such mixed phase is composed by the chiral and 2SC phases while for $T > T_{3P}$ it is a mixture of the chiral and the free quark gas phases.

As for the comparison between the results of Set I and II, we see that they are qualitatively very similar, with only small quantitative differences in the position of the critical points.

III.2 Lorentzian regulator

The Lorentzian regulator we have considered has the form

$$r(p^2) = \frac{1}{1 + p^2/\Lambda^2}. \tag{21}$$

The input parameters are $G = 28.38\ GeV^{-2}$, $m_c = 4.57\ MeV$, $\Lambda = 940\ MeV$. Once again, we have solved the gap equations for different values of the temperature and chemical potential. The qualitative behavior of the mean field values and condensates is very similar to that found using the Gaussian regulator (Fig.1) and, thus, will not be explicitly shown. Nevertheless it is interesting to note that, as shown in Table 1, in this case the $T = 0$ diquark gap at the critical chemical potential $\bar{\Delta}_c$ is somewhat smaller. The corresponding phase diagrams in the $T - \mu$ and $T - \rho/\rho_0$ planes are displayed in Fig.3. As in the previous cases, we observe the existence of an "end point", at which the first order chiral phase transition line becomes a crossover line, and a triple point at which the three phases co-exist. The position of these points, which are quite similar to those of the Gaussian regulator Set II, are given in Table 1.

IV Dependence of the phase diagrams on the diquark coupling constant

In the previous section we have assumed $H/G = 3/4$ as favored by various effective models of quark-quark interactions. However, this value is subject to rather large uncertainties. In fact, so far there is no strong phenomenological constrain on the ratio H/G. Thus, it is worthwhile to explore the consequences of varying H/G in the range $0 < H/G \leq 1$. Larger values of this ratio are quite unlikely to be realized in QCD and might lead to color symmetry breaking in the vacuum. Since the results obtained above for different regulators are qualitatively very similar in what follows we will only consider the Gaussian regulator with the set of parameters Set II.

For values of H/G in the range $0.17 < H/G < 0.82$ the resulting phase diagrams look qualitatively similar to the one displayed in Fig.2, although the details (in particular the position of the critical points, see below) do depend on H/G. For $H/G < 0.17$ there is a qualitative change since the triple point ceases to exist. In this case, even at very low temperatures, as we increase μ at some point we find a first order phase transition between the chiral phase and the free quark gas phase. For values slightly above this critical μ we have $\bar{\sigma} \simeq \bar{\Delta} = 0$. If we continue to increase μ we find a second order phase transition between the free quark gas phase and the 2SC phase. The corresponding $T - \mu$ phase diagram is shown in the upper panel of Fig.4. Note that in this phase diagram the transition line between the chiral and the free quark gas phases (both its crossover and first order sections) coincides exactly to the one obtained for $H = 0$. For $H/G > 0.82$ the situation is again qualitatively different, since in such range the triple point and the end point

merge together. In fact, as H/G comes closer from below to $H/G = 0.82$ the first order transition line that connects the 3P and the EP becomes shorter and shorter and at this particular value it disappears. Moreover, for $H/G > 0.82$ there is small region at low temperatures at which both $\bar{\sigma}$ and $\bar{\Delta}$ take non-vanishing values. This region is separated from the chiral phase by a second order transition line and from the 2SC for a first order transition line. This situation is illustrated in the lower panel of Fig.4 where the $T - \mu$ phase diagram for $H/G = 0.90$ is shown. The possible existence of this type of phase was already noticed in Refs.[15, 16].

The behavior of the critical points as function of H/G is displayed in Fig.5. In the upper panel we show the position of critical chemical potential μ_c at $T = 0$. The full line indicates the first order μ_c while the dashed line the second order one. In the range $0.17 < H/G < 0.82$ we have only a first order μ_c. For values below such μ_c the system is in the chiral phase while for values above is in the 2SC. For values $H/G < 0.17$ we have that the second order μ_c, i.e. the point at which the second order transition line that separates the 2SC and free quark gas phases meets the μ-axis in the $T - \mu$ phase diagram, grows rather fast as H/G decreases, signaling the almost disappearance of the 2SC phase for very small values of the diquark coupling constant. For $H/G > 0.82$ a second order μ_c appears again, but now *below* the first order μ_c. Thus, between these two critical chemical potentials we have $\bar{\sigma} \neq 0$ *and* $\bar{\Delta} \neq 0$. In the lower panel we display the position of the triple and end points as functions of H/G. Note that the temperature scale is given to the right while the chemical potential scale is given to the left. For values of $H/G < 0.17$ only the the EP exists. Its positions remains independent of the diquark coupling constant up to $H/G = 0.82$ where it meets the 3P, that appears at $H/G = 0.19$ and which position in temperature (chemical potential) increases (decreases) as H/G increases. For values of $H/G > 0.82$ both critical points transform into a single one which position in temperature (chemical potential) increases (decreases) as H/G increases.

V Conclusions

In this work we have studied the finite temperature and chemical potential behavior of $SU(2)_f$ chiral quark models with nonlocal covariant separable interactions in both the scalar quark-antiquark and quark-quark channels. In our numerical calculations we have considered two types of regulators: the Gaussian regulator and the Lorentzian regulator. In all these cases we have set the model parameters so as to reproduce the empirical values of the pion mass and decay constant and to get a chiral quark condensate in reasonable agreement to that determined from lattice gauge theory or QCD sum rules. As for the ratio between quark-quark and quark-antiquark interactions H/G which is not well constrained by phenomenology, we have in principle adopted the standard value $H/G = 3/4$ which follows from some models of the QCD interactions. We find that in all cases the phase diagram is quite similar. In particular, we obtain that for two light flavors there are always two critical points: a "triple point" at which the second order transition line separating the 2SC and normal phases meets the first order transition line which separate the chiral and 2SC phases at low temperatures; an "end point" which appears at higher temperatures and at which the first order transition line becomes a crossover line. Of course, there is also a critical temperature $T_c(\mu = 0)$ above which the chiral condensate always vanishes. As displayed in Table 1 the values of $T_c(\mu = 0)$ are in the range $115 - 120$ MeV, that is somewhat below the values obtained in modern lattice simulations which suggest $T_c(\mu = 0) \approx 140 - 190$ MeV[4]. With this in mind we note that our

predictions for the positions of the triple and end points are very similar for all the cases considered. Perhaps, the only noticeable difference between the different cases is the prediction for the $T = 0$ diquark gap at the critical chemical potential, where we find values that range from 114 to 182 MeV. These values are larger than those obtained within models with instantaneous interactions [2]. It should be noticed (see Fig.1) that in the present case the diquark gap also registers a stronger increase with μ after the phase transition. This leads to rather large values of the gap for chemical potentials of the order of 400 MeV, above which strange degrees of freedom have to be taken into account. Consequently, for such values of μ, we also get larger values (100-120 MeV) for the critical temperature needed to go to the free quark gas phase, as it can be easily seen comparing our phase diagrams with those obtained in e.g. the NJL model[7, 16].

In the final part of this work we have explored the consequences of varying H/G in the range $0 < H/G \leq 1$. Given the similarity of the results obtained for the two regulators mentioned above we have considered here only the Gaussian regulator with the set of parameters Set II. We found that for $H/G < 0.17$ there is no triple point. On the other hand, for $H/G > 0.82$ the triple and end point merge and a phase where both the chiral and diquark condensates are non-negligible appears. It is interesting to remark that the value $H/G = 0.82$ is quite close to the standard one $H/G = 0.75$ used in most model calculations. Thus, it would be important to sort out possible phenomenological consequences of having quark matter with a phase diagram in which the 3P and EP coincide.

In this work we have neglected the strangeness degrees of freedom. To go beyond the values of chemical potential considered here and, thus, study for example the Color Flavor Locked phase in the context of models with non local interactions their effect have to be included. Work in this direction is in progress.

Acknowledgements

We thank D. Blaschke and D. Gómez Dumm for useful discussions. This work has been partially supported by CONICET and ANPCyT under grants PIP 02368 and PICT 00-03-08580, respectively.

References

[1] B. C. Barrois, Nucl. Phys. **B129**, 390 (1977); S.C. Frautschi, in "Hadronic matter at extreme energy density", edited by N. Cabibbo and L. Sertorio (Plenum Press, 1980); D. Bailin and A. Love, Phys. Rep. **107**, 325 (1984).

[2] K. Rajagopal and F. Wilczek, in *At the Frontier of Particle Physics / Handbook of QCD*, M. Shifman, ed. (World Scientific, Singapore, 2001); M. Alford, Annu. Rev. Nucl. Part. Sci. 51, 131 (2001); D. H. Rischke, Prog. Part. Nucl. Phys. **52**, 197 (2004).

[3] M. Alford, K. Rajagopal and F. Wilczek, Phys. Lett. **B422**, 247 (1998); R. Rapp, T. Schäfer, E.V. Schuryak and M. Velkovsky, Phys. Rev. Lett. **81**, 53 (1998).

[4] F. Karsch and E. Laermann, arXiv:hep-lat/0305025.

[5] Y. Nambu and G. Jona-Lasinio, Phys. Rev. **122**, 345 (1961); Phys. Rev. **124**, 246 (1961).

[6] U. Vogl and W. Weise, Prog. Part. Nucl. Phys. **27**, 195 (1991); S. Klevansky, Rev. Mod. Phys. **64**, 649 (1992); T. Hatsuda and T. Kunihiro, Phys. Rep. **247**, 221 (1994).

[7] M. Buballa, arXiv:hep-ph/0402234.

[8] G. Ripka, *Quarks bound by chiral fields* (Oxford University Press, Oxford, 1997).

[9] T. Schäfer and E.V. Schuryak, Rev. Mod. Phys. **70**, 323 (1998).

[10] C.D. Roberts and A.G. Williams, Prog. Part. Nucl. Phys. **33**, 477 (1994); C.D. Roberts and S.M. Schmidt, Prog. Part. Nucl. Phys. **45**, S1 (2000).

[11] R.D. Bowler and M.C. Birse, Nucl. Phys. **A582**, 655 (1995); R.S.Plant and M.C. Birse, Nucl. Phys. **A628**, 607 (1998).

[12] W. Broniowski, B. Golli and G. Ripka, Nucl. Phys. **A703**, 667 (2002); A.H. Rezaeian, N.R. Walet and M.C. Birse, arXiv:hep-ph/0408233.

[13] A. Scarpettini, D. Gómez Dumm and N.N. Scoccola, Phys. Rev. **D69**,114018 (2004).

[14] I. General, D. Gómez Dumm, N.N. Scoccola, Phys. Lett. B **506**, 267 (2001); D. Gómez Dumm, N.N. Scoccola, Phys. Rev. D **65**, 074021 (2002).

[15] R. Rapp, T. Schäfer, E. V. Shuryak and M. Velkovsky, Annals Phys. **280**, 35 (2000)

[16] D. Blaschke, M.K. Volkov and V.L. Yudichev, Eur. Phys. J. **A17**, 103 (2003)

Regulator	Triple Point		End Point		$T_c(\mu = 0)$	$\bar{\Delta}_c(T = 0)$
	T_{3P}	μ_{3P}	T_{EP}	μ_{EP}		
Gaussian - Set I	64	193	69	180	115	182
Gaussian - Set II	54	215	58	207	120	132
Lorentzian	48	217	59	195	116	114

Table 1: Critical temperatures, chemical potentials and $\bar{\Delta}_c(T = 0)$ (all in MeV) for different regulators.

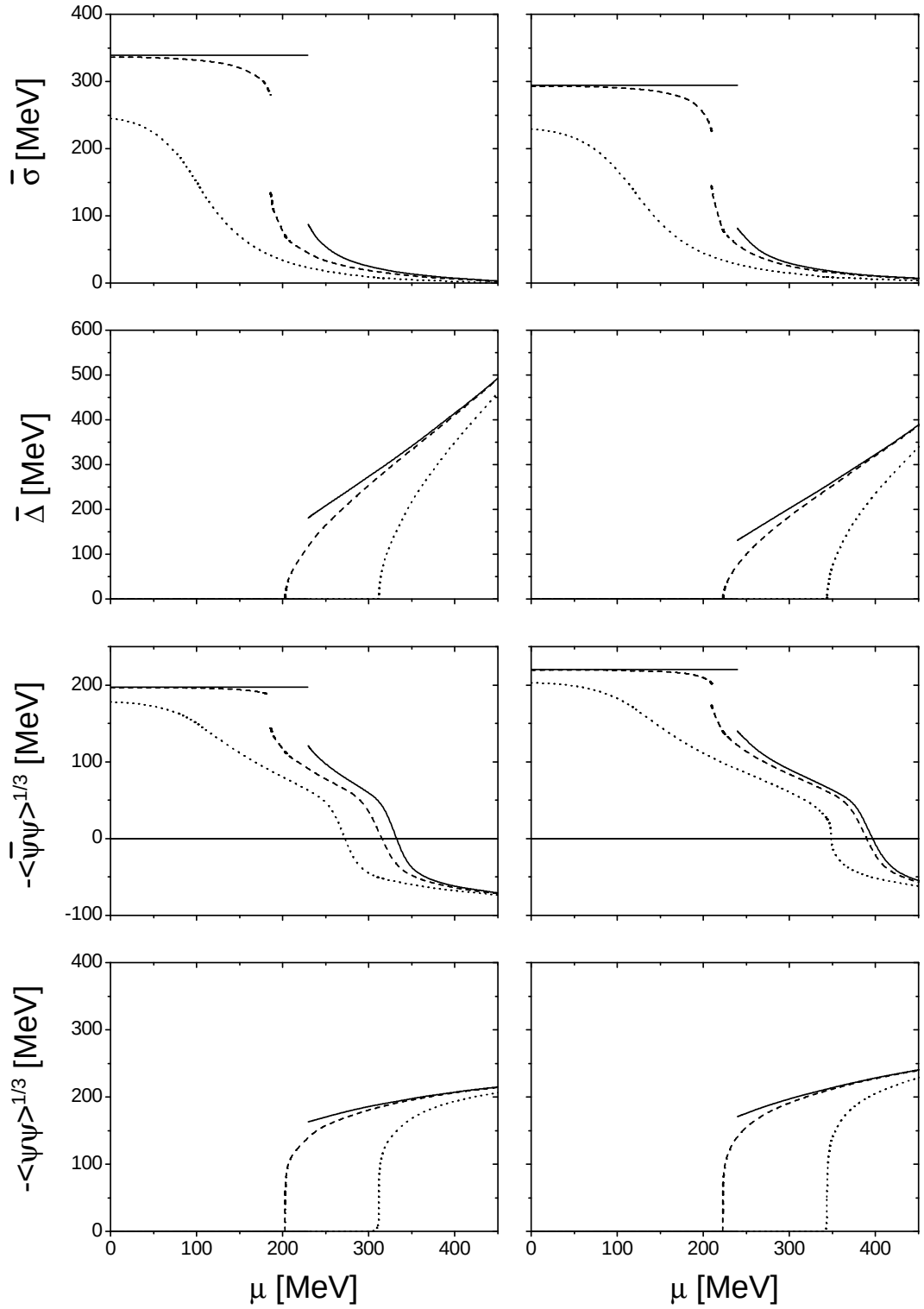

Figure 1: Behavior of mean fields $\bar{\sigma}$, $\bar{\Delta}$ and condensates $\langle\bar{q}q\rangle$, $\langle qq\rangle$ for the Gaussian regulator, as a function of chemical potential for three different values of the temperature. Left panels correspond to Set I and right ones to Set II. Full lines correspond to $T = 0$, dashed lines to $T = 67MeV$ for Set I ($T = 57MeV$ for Set II) and dotted lines to $T = 100MeV$.

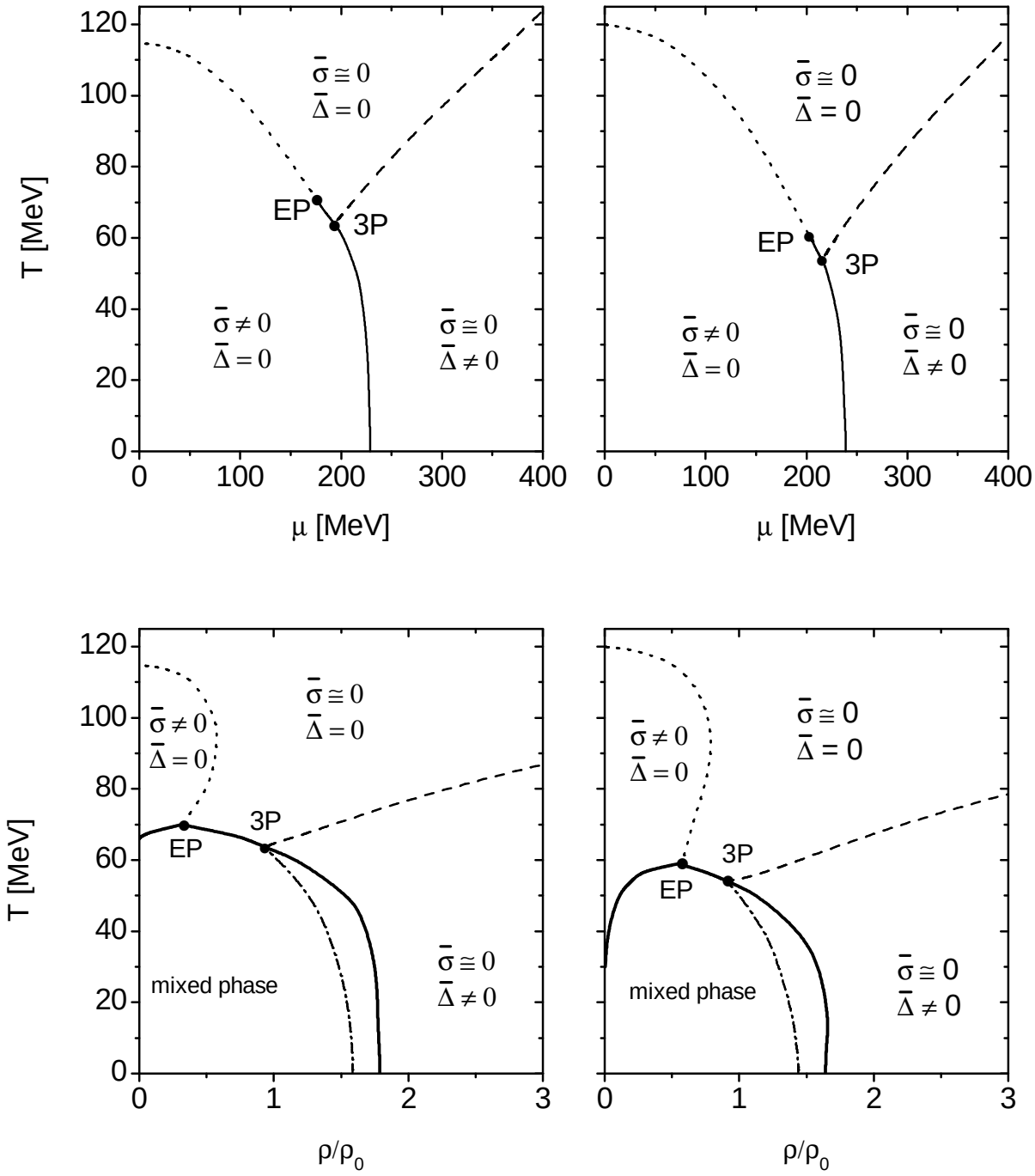

Figure 2: Phase diagrams for the Gaussian regulator. Left panels correspond to Set I and right ones to Set II. Upper panels display the $T-\mu$ phase diagrams and the lower ones the $T-\rho/\rho_0$ phase diagrams. Full lines indicate first order transition lines, dashed lines correspond to second order transition lines and dotted lines to crossover lines. The dash-dotted line in the lower panels indicates the section of the transition line corresponding to $H=0$.

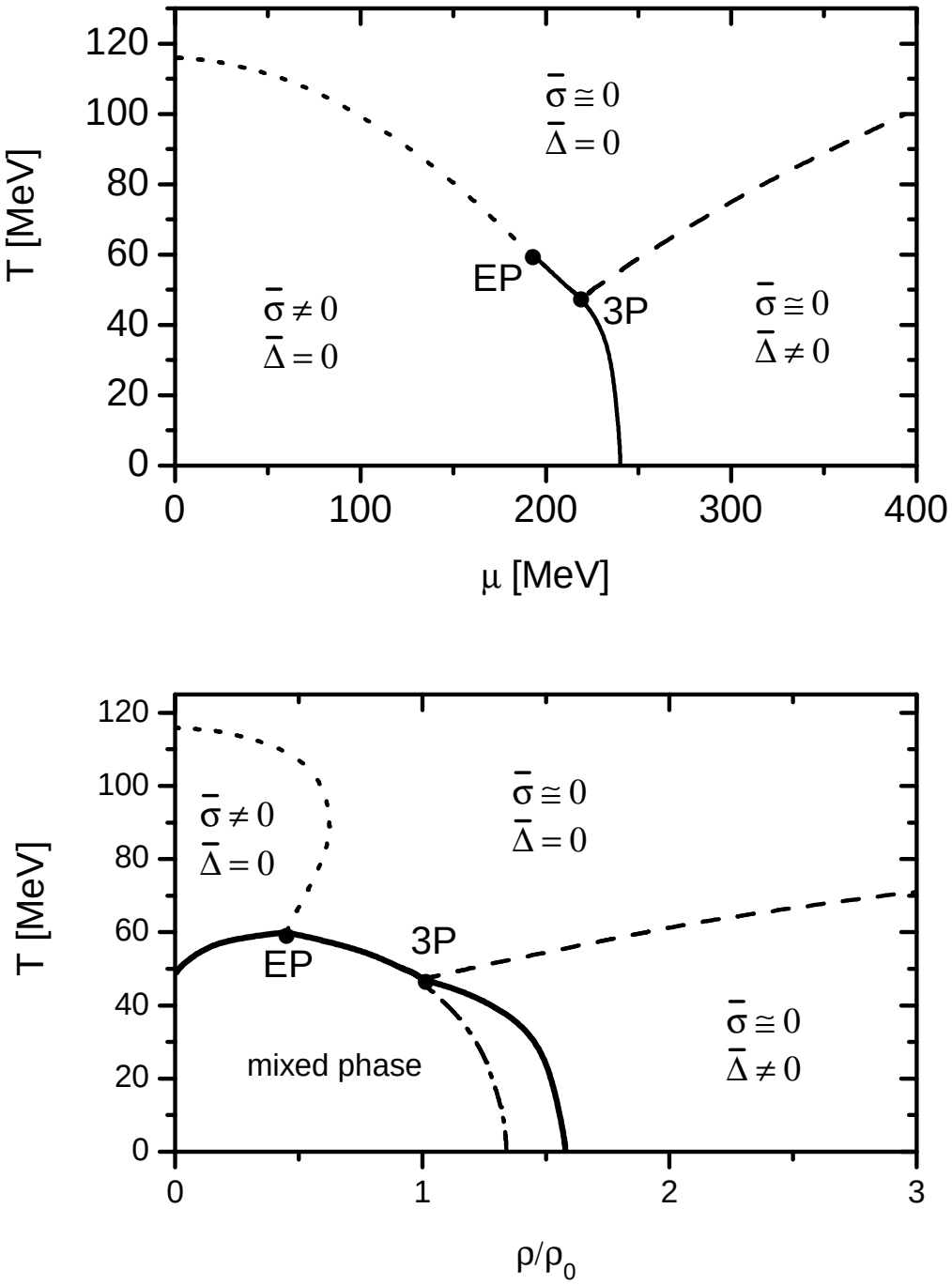

Figure 3: Phase diagrams for the Lorentzian regulator. Upper panels display the $T-\mu$ phase diagrams and the lower ones the $T-\rho/\rho_0$ phase diagrams. Full lines indicate first order transition lines, dashed lines correspond to second order transition lines and dotted lines to crossover lines. The dash-dotted line in the lower panels indicates the section of the transition line corresponding to $H=0$.

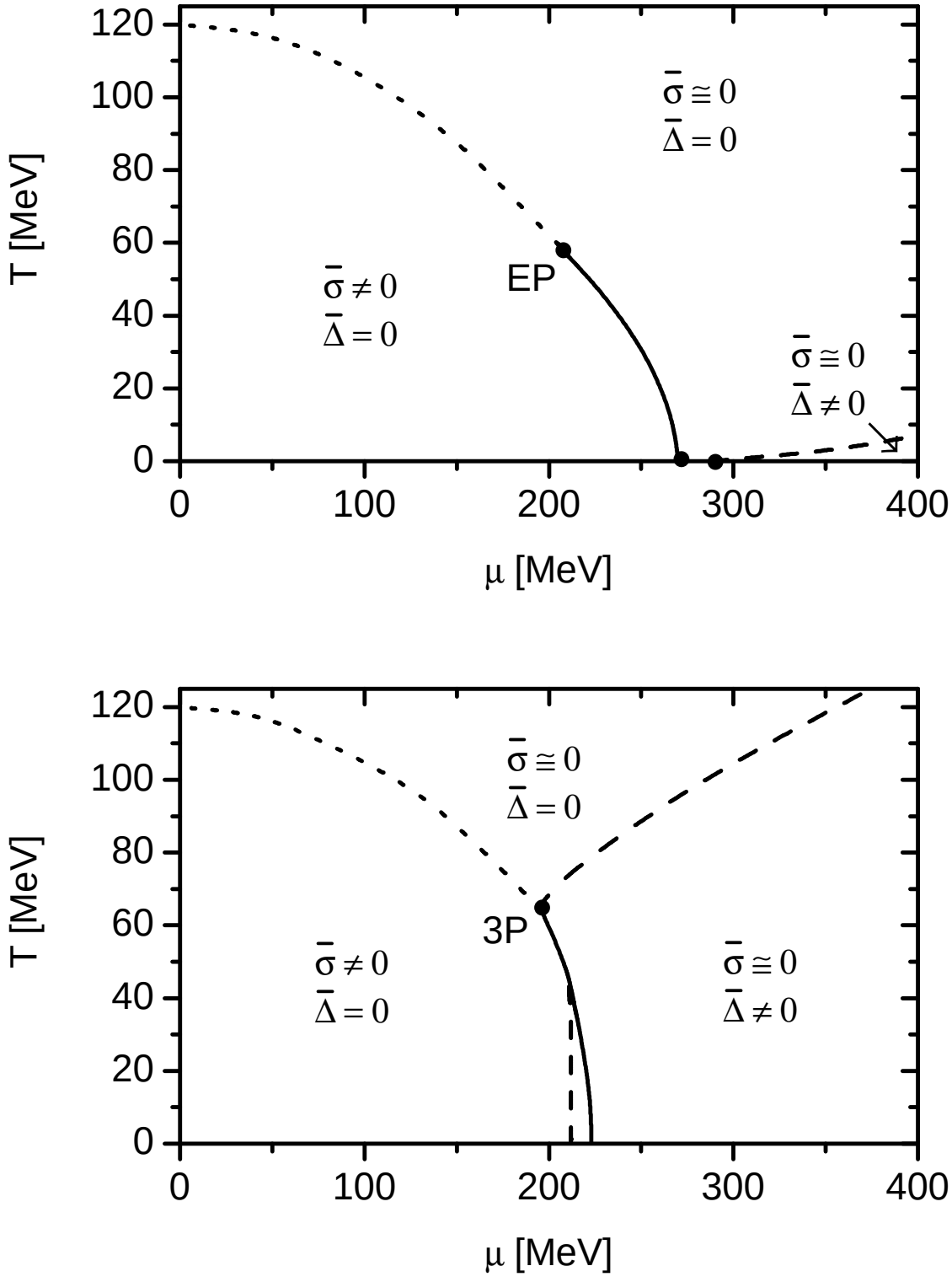

Figure 4: Phase diagrams for the Gaussian regulator (Set II) and different values of the ratio H/G. The upper panel corresponds to the ratio $H/G = 0.15$ while the lower one to $H/G = 0.9$.

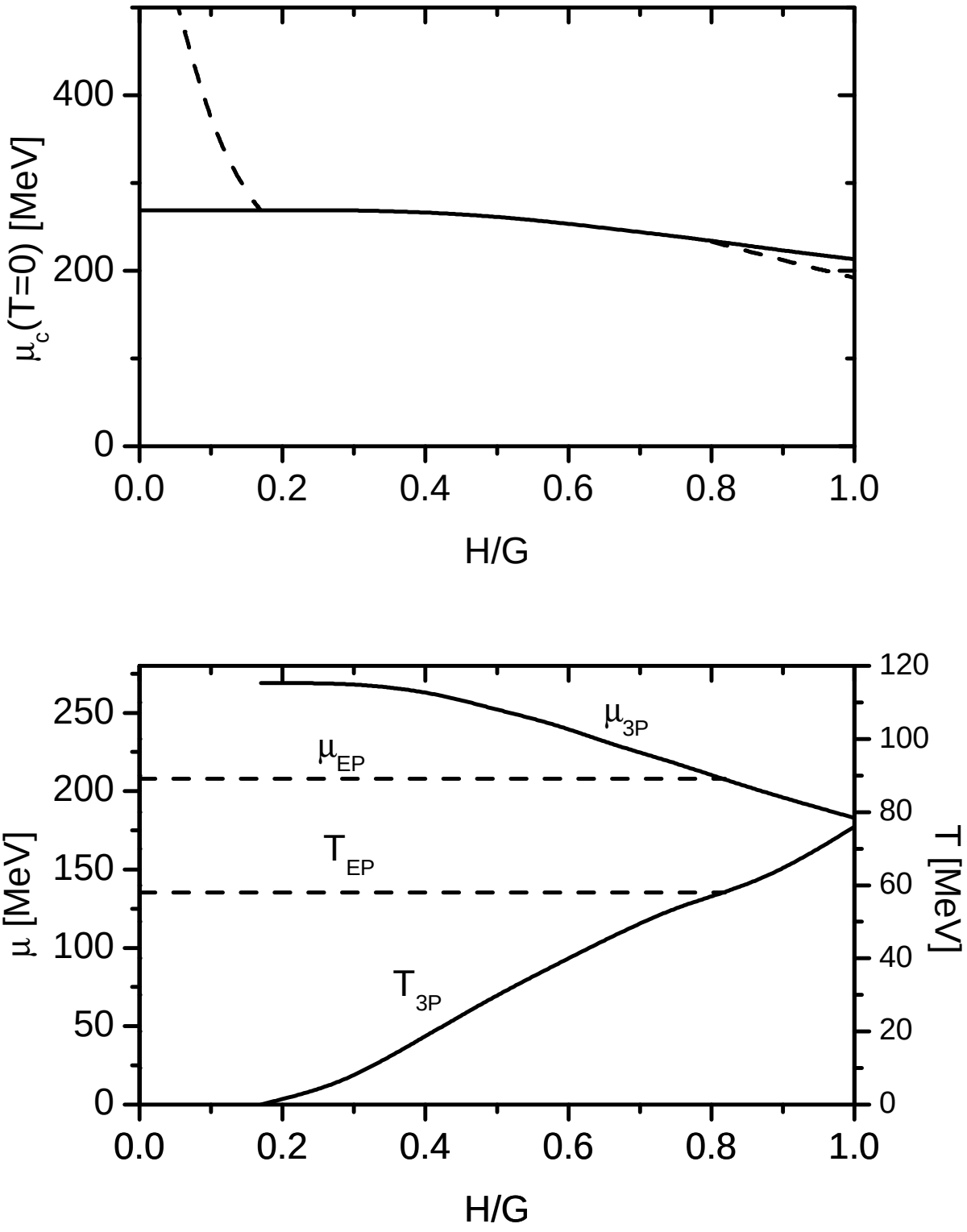

Figure 5: Behavior of the critical points for the Gaussian regulator (Set II) as a function of H/G. The upper panel displays the critical chemical potentials at $T = 0$. The lower panel shows the position of the triple and end points.